

# **Ionic Conductivity in Glasses and Melts (Up to 1950 K): Application to the CaO–SiO<sub>2</sub> System<sup>1</sup>**

**M. Malki<sup>2-4</sup> and P. Echegut<sup>2</sup>**

---

The electrical properties of the CaO–SiO<sub>2</sub> system have been investigated in a wide temperature range (up to 1950 K) using a specific device developed in this laboratory. Conductivity data were obtained in the liquid, undercooled-liquid, and glassy states for two different compositions. In the solid state, the conductivity is determined by the jump of the Ca<sup>2+</sup> cations along the non-bridging oxygens. This mechanism is thermally activated with a high activation energy value. A second regime was observed in the molten state where the conductivity follows the phenomenological Vogel–Tammann–Fulcher (VTF) law. In this regime, the conductivity is enhanced because the softening and the deformation of the network facilitate the migration of the alkaline-earth cations.

---

**KEY WORDS:** CaO–SiO<sub>2</sub> system; electrical conductivity; glass; melt; high temperature.

## **1. INTRODUCTION**

While the electrical conductivity of solid glasses has been extensively studied, only a few studies have been devoted to the charge transport in glass-forming melts at high temperature. The most common method uses an alumina tube for which the extremities are painted with platinum and used as electrodes. [1] This type of cell, although simple in principle, has a major drawback because alumina may interact with liquid oxides and then

---

<sup>1</sup>Paper presented at the Fifteenth Symposium on Thermophysical Properties, June 22–27, 2003, Boulder, Colorado, U.S.A.

<sup>2</sup>CRMHT-CNRS-Orléans, 1D, avenue de la Recherche Scientifique, 45071 Orléans cedex 02, France.

<sup>3</sup>Polytech'Orléans-Université d'Orléans, 8, rue Léonard de Vinci, 45072 Orléans cedex 02, France.

<sup>4</sup>To whom correspondence should be addressed. E-mail: mohammed.malki@univ-orleans.fr

change their composition. To avoid this contamination, some investigators [2, 3] used a platinum crucible and inserted two platinum wires (electrodes) in the melt. The geometric factor of the cell is then obtained by a calibration with a standard ionic solution whose conductivity is well known. However, in the two-electrode method, the data are generally influenced by the polarization effects due to the charge accumulation near the electrodes. [4]

In order to obtain accurate data in the molten state, we built an original device able to perform conductivity measurements at high temperature (up to 1950 K) over a wide frequency range (100 Hz–1 MHz). This device has been applied to study the transport mechanism in the molten and undercooled states of the alkaline-earth silicate system CaO–SiO<sub>2</sub>. Furthermore, a calibration-free technique has been used in order to carry out the conductivity measurements in the solid state from 750 to 1250 K. While alkali silicate glasses have been considerably investigated, only a small number of studies on alkaline earth silicate glasses have been reported to date. This is mainly due to the difficulty of obtaining the glassy state in these systems. For example, for the CaO–SiO<sub>2</sub> system, a temperature as high as 1950 K is needed to obtain a homogenous melt and a high quenching rate is necessary to avoid crystallization.

## 2. EXPERIMENTAL

### 2.1. Sample Preparation

Two compositions in the  $x$  CaO – (1- $x$ ) SiO<sub>2</sub> system with  $x=44$  and 50 mol% were prepared by mixing pre-dried SiO<sub>2</sub> (99.99%) and CaCO<sub>3</sub> (99.95%) powders in the correct proportions. For each sample, the mixture was melted in a Pt crucible at 1950 K for 2 h, and quenched by placing the bottom of the crucible in water. The glass was transparent and free of crystallization as confirmed by the absence of Bragg peaks in XRD spectra. The glass transition temperature  $T_g$  (Table I) was determined by differential scanning calorimetry (DSC) at a heating rate of 10 K·min<sup>-1</sup>. The values of  $T_g$  are in good agreement with those reported by Shelby [5] using the dilatometric technique.

### 2.2. Solid-State Measurements

In the glassy state, the electrical conductivity was measured in the temperature range 750–1250 K and the frequency range 100 Hz–10 MHz using a HP4194A impedance spectrometer and a LabView program for data acquisition. The samples were 0.5 cm<sup>2</sup> glass pellets with a thickness

**Table I.** Glass Transition Temperatures  $T_g$ , and Arrhenius and VTF Parameters of the  $x$  CaO – (1– $x$ ) SiO<sub>2</sub> System in Solid and Molten States

Composition	0.44 CaO–0.56 SiO <sub>2</sub>	0.50 CaO–0.50 SiO <sub>2</sub>
$T_g$ (K)	1043 ± 3	1053 ± 3
$E$ (kJ.mol. <sup>-1</sup> )	137 ± 2	132 ± 2
$A$ ( $\Omega^{-1}$ . cm <sup>-1</sup> .K)	1940 ± 10	3300 ± 10
$\Delta$ (kJ mol <sup>-1</sup> )	23.1 ± 0.4	23.1 ± 0.4
$T_0$ (K)	1026 ± 5	1053 ± 5

of about 1 mm. Platinum was evaporated as electrodes on both faces of the pellet. The temperature was measured by a Pt/Pt–10%Rh thermocouple located about 1 mm from the sample.

### 2.3. Molten-State Measurements

An original device for electrical conductivity measurements in the molten state was developed in our laboratory to obtain conductivity data up to 1950 K over a wide frequency domain. This setup is based on the four-electrode method in order to reduce the electrode polarization effects usually observed in the two-point classical method, particularly at high temperatures and low frequencies. The cell details are shown in Fig. 1. Further details about the experimental setup, calibration, and corrections are given elsewhere. [6,7] The melt is contained in a Pt crucible placed in the middle of a vertical tubular furnace. The electrode system consists of two Pt wires (2 and 3) for voltage drop ( $U$ ) measurements and two Pt sheets (1 and 4) for current ( $I$ ) measurements. The electrodes are mechanically linked to a micrometer displacement system, which allows the depth determination with good precision. The complex impedance of the melt is measured in the frequency range 100 Hz–1 MHz with the same impedance spectrometer as in the solid state. The temperature measurement is performed with a Pt/Pt–10%Rh thermocouple located about 2 mm above the melt surface. A KCl 1 M solution whose conductivity is well known, [8] is used for the cell calibration at room temperature.

## 3. RESULTS

### 3.1. Solid State

The complex electrical conductivity was measured in the two glasses upon heating from 750 to 1250 K in steps of 20 K in the frequency range

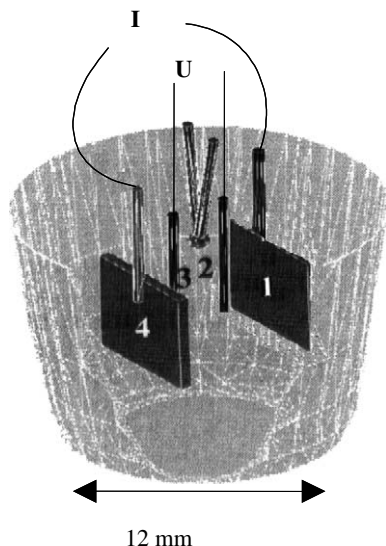


**Fig. 1.** Platinum crucible and electrode assembly: (1) and (4) are the current electrodes and (2) and (3) are the voltage electrodes.

100 Hz–10 MHz. The high temperature part is restricted to 1250 K because of the softening and crystallization of the sample. On the other hand, the low temperature part is restricted to 750 K because of the very large impedance of the sample (about  $10^{10} \Omega$ ), which cannot be measured with high accuracy with the bridge. The complex impedance was plotted in the Cole–Cole representation ( $-Z''$  vs.  $Z'$ ) for the complete set of measurements. At a given temperature, the plot is a circular arc with the center located slightly below the real axis (Fig. 2). The dc-conductivity  $\sigma$  of the sample is determined using the upper-side intersection of this arc with the real axis ( $Z'' = 0$ ) [9]. The evolution of the  $\sigma T$  product as a function of temperature in Arrhenius coordinates is given in Fig. 3. The curve exhibits a clear crossover occurring around the glass transition temperature  $T_g$ . Below  $T_g$ , the  $\sigma T$  product follows a straight-line characteristic of thermally activated transport:

$$\sigma T = A \exp\left(-\frac{E}{kT}\right) \quad (1)$$

where  $E$  is the activation energy,  $A$  is the pre-exponential factor, and  $k$  is the Boltzmann constant. In Table I are listed the values of the activation energy as well as the values of the pre-factor  $A$  for the two studied glasses.

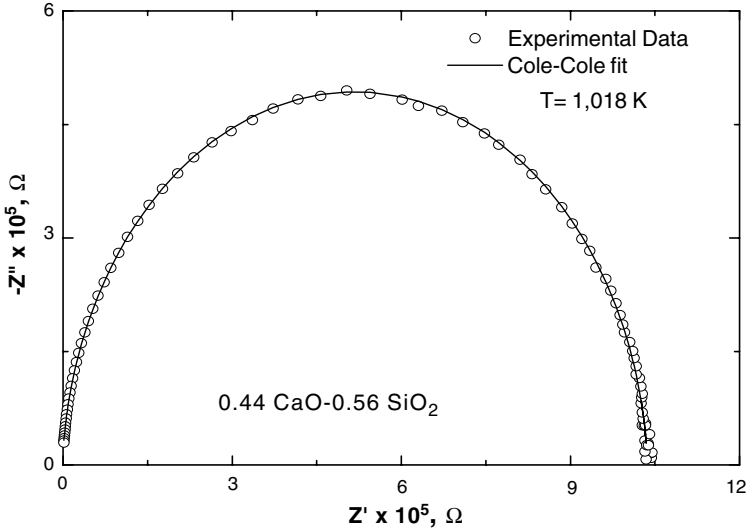


**Fig. 2.** Cole–Cole plot of the complex impedance for the 0.44 CaO–0.56 SiO<sub>2</sub> glass at  $T = 1018$  K. Circles are the experimental points, the solid line is the best fit with a circular arc.

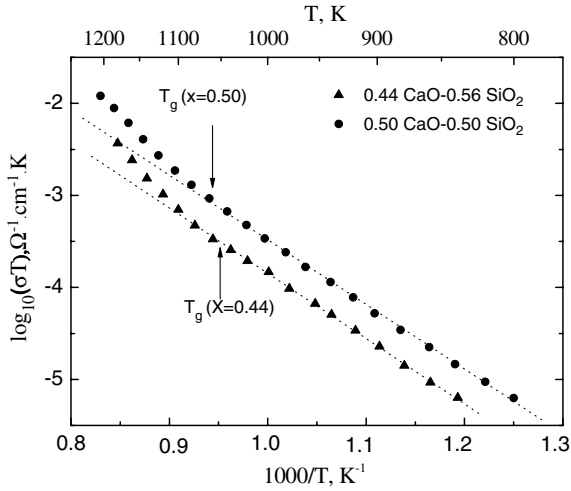


**Fig. 3.** Arrhenius plot of the  $\sigma T$  product below and above the glass transition temperature  $T_g$ .

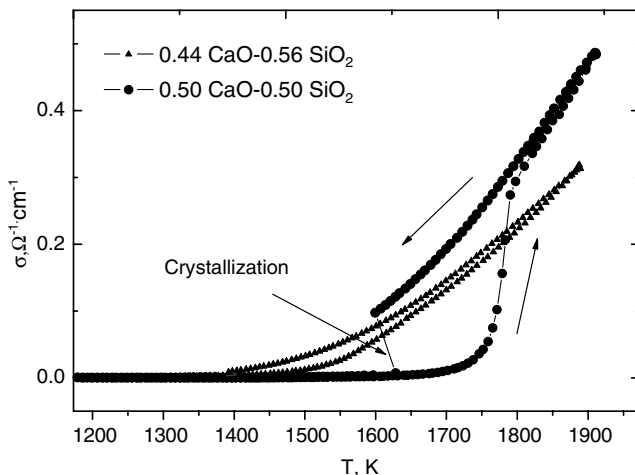
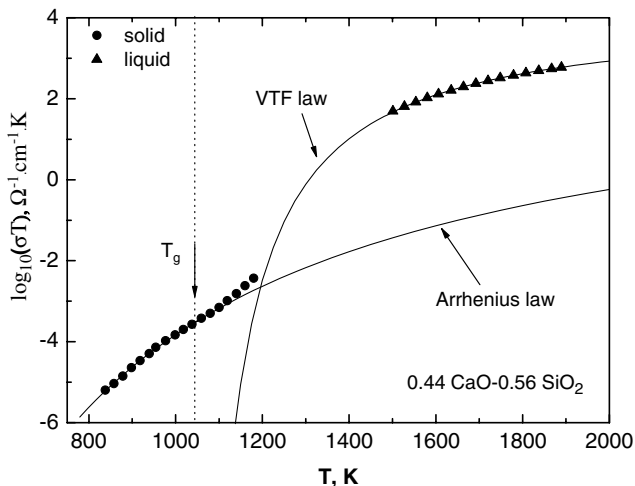


Fig. 4. Electrical conductivity data during a temperature cycle obtained with the molten-state setup.

### 3.2. Molten State

The solid-state measurements showed the onset of a non-Arrhenius conductivity regime above the glass transition temperature. In order to complete the data above  $T_g$  and in the molten state, we used our specific four-electrode setup. For each sample, the conductivity measurements were performed during a cycle from 1950 K down to 1200 K with a cooling rate of  $150 \text{ K}\cdot\text{h}^{-1}$ , then on heating the sample to 1950 K. At a constant temperature, the electrical conductivity was almost frequency-independent in the range [100 Hz–1 MHz]. The data obtained during this cycle are plotted in Fig. 4 for  $x = 44$  and 50 mol% melts. We can see an important hysteresis loop in the case of the 0.50 CaO – 0.50 SiO<sub>2</sub> sample. Moreover, a large undercooling interval (190 K) is observed at this slow cooling rate followed by the onset of crystallization at 1600 K, where the conductivity decreases suddenly by more than one decade. An elevation of the sample temperature ( $\Delta T = 30 \text{ K}$ ) was also noticed during the crystallization process although the furnace was programmed for cooling. Upon heating, the conductivity increases strongly just below the melting temperature ( $T_m = 1817 \text{ K}$ ) and then reaches the previous values (on cooling) in the molten state. The cycle corresponding to the 0.44 CaO – 0.56 SiO<sub>2</sub> sample is very narrow compared to the 0.5 CaO – 0.5 SiO<sub>2</sub> results. This behavior reveals the relative high tendency for the 0.44 CaO – 0.56 SiO<sub>2</sub> melt to vitrify even at a slow cooling rate.



**Fig. 5.** Temperature dependence of the electrical conductivity of the 0.44 CaO–0.56 SiO<sub>2</sub> system showing the two types of behavior in the solid and molten states. The solid lines are the best fits with the Arrhenius and VTF laws.

We consider now the conductivity dependence vs. temperature only in the liquid and undercooled states. In this temperature range, we were not able to fit the conductivity data with a simple Arrhenius law, but we obtained an excellent fit using the phenomenological Vogel–Tammann–Fulcher (VTF) law:

$$\sigma T = B \exp \left[ -\frac{\Delta}{k(T - T_0)} \right] \quad (2)$$

where  $B$  is a constant related to the charge carriers concentration,  $\Delta$  is a pseudo-activation energy, and  $T_0$  is a temperature called the ideal glass transition. The VTF fit parameters are listed in Table I for each sample.

#### 4. DISCUSSION

The use of the solid state setup and the original molten state setup allowed us to measure the electrical conductivity of the CaO – SiO<sub>2</sub> system in a wide temperature range (750 to 1950 K). We followed the conductivity behavior in several states of this system: liquid, undercooled liquid, and glass. Figure 5 summarizes the data obtained for the 0.44 CaO – 0.56 SiO<sub>2</sub> system (see also Table I).

Some authors suggested that in the absence of alkali cations, it should be very difficult to observe the motion of divalent cations below  $T_g$ . [10] Our results, however, show clearly a non-negligible conductivity in the pure alkaline-earth silicate glass even at low temperatures ( $\sigma \approx 10^{-8} \Omega^{-1} \cdot \text{cm}^{-1}$  at  $T \approx 820 \text{ K}$ ). Below the glass transition temperature  $T_g$ , the electrical conductivity follows an Arrhenius behavior (Fig. 5), which is characteristic of thermally activated transport. In the studied glasses, each  $\text{Ca}^{2+}$  cation creates two non-bridging oxygens (NBO) and the ionic conductivity is ensured by the jump of the alkaline earth cations along these NBO. The activation energy values (Table I) found in this study are in agreement with those reported by Gruener et al. [11] in the ternary system  $\text{CaO} - \text{SiO}_2 - \text{Al}_2\text{O}_3$  with a small amount of alumina, but they are twice as large as the typical values of the alkali silicate glasses. [12] One can expect that the divalent character of the  $\text{Ca}^{2+}$  cations results in a large binding energy of these cations to non-bridging oxygens.

In the molten state, the conductivity rises faster than the Arrhenius law because of the softening and deformation of the network, which enhances the diffusion of the charge carriers. The transport mechanism become cooperative ( $\text{Ca}^{2+}$  cations/network) and the conductivity is well described by the VTF law (Fig. 5). This phenomenological law, which is commonly used to describe the temperature dependence of the viscosity for fragile silicate melts, [13] can be deduced from the free-volume theory. [14] Using the concept introduced by Rössler et al., [15] we can calculate the fragility parameter  $F = T_x / (T_x - T_g)$  for both glasses. Indeed, taking  $T_x$  as the crossover temperature from the Arrhenius to the VTF regime, we obtain  $F = 7.7$  and  $7.2$  for  $x = 44$  and  $50 \text{ mol}\%$  respectively.

Recently, Souquet et al. [16] developed a model, which gives a more precise image to explain the VTF behavior for the conductivity in alkali silicate melts. According to this model, the enhancement of the conductivity results from the local deformations of the macromolecular chains or network above  $T_g$ . These deformations, which need local fluctuations of free volume, facilitate the jump of cations along the NBO.

As in the solid state, the electrical conductivity of the  $\text{CaO-SiO}_2$  melt is small compared to the alkali silicate melt conductivity at a given temperature. The difference can be attributed to the high value of the pseudo-activation energy  $\Delta$  term (Table I). For example, in the  $\text{K}_2\text{O} - 2 \text{SiO}_2$  melt,  $\Delta$  is about  $10 \text{ kJ} \cdot \text{mol}^{-1}$  from the study carried out by Caillot et al. [17]

The analysis of Table I shows the increase of the conductivity with calcium content in the solid state as well as in the molten state. However, in order to study the complete influence of the Ca concentration on the conductivity, more compositions are needed.



## 5. CONCLUSION

In order to obtain electrical conductivity data in oxides from room temperature up to 1950 K, we developed an original setup based on the four-electrode method. This setup has been successfully applied to study the ionic mobility in the alkaline-earth silicate system CaO – SiO<sub>2</sub> from the solid state to the molten state. Below the glass transition temperature  $T_g$ , the transport mechanism is thermally activated with a high activation energy value. In the molten state, the deformation of the network enhances the diffusion of the Ca<sup>2+</sup> cations and the conductivity is well described by the phenomenological Vogel–Tammann–Fulcher (VTF) law.

## REFERENCES

1. F. G. K. Baucke, J. Braun, G. Röth, and R. D. Werner, *Glasstech. Ber.* **62**:122 (1989).
2. J. O. M. Bockris, J. A. Kitchener, S. Ignatowics, and J. W. Tomlinson, *Faraday Soc. Discuss.* **6**:265 (1948).
3. W. C. Hasz and C. T. Monyhan, *Mater. Sci. Forum* **67**:55 (1991).
4. W. B. Reid, E. E. Lachowski, and A. R. West, *Phys. Chem. Glasses* **31**:103 (1990).
5. J. E. Shelby, *J. Appl. Phys.* **50**:8010 (1979).
6. M. Malki and P. Echegut, *J. Non-Cryst. Solids* **323**:131 (2003).
7. C. Simonnet, J. Phalippou, M. Malki, and A. Grandjean, *Rev. Sci. Instrum.* **74**:2805 (2003).
8. Y. C. Wu and W. F. Koch, *J. Solution Chem.* **20**:4 (1991).
9. A. K. Jonscher, *Dielectric Relaxation in Solids* (Chelsea Dielectric Press, London, 1983).
10. B. Roling and M. Ingram, *J. Non-Cryst. Solids* **265**:113 (2000).
11. G. Gruener, D. De Sousa Meneses, P. Odier, and J. P. Loup, *J. Non-Cryst. Solids* **281**:117 (2001).
12. R. M. Hakim and D. R. Uhlmann, *Phys. Chem. Glasses* **12**:132 (1971).
13. T. Pfeifer, *Solid State Ionics* **105**:277 (1998).
14. Y. Bottinga, P. Richet, and A. Sipp, *Am. Mineral.* **80**:305 (1995).
15. E. Rössler, K. U. Hess, and V. N. Novikov, *J. Non-Cryst. Solids* **223**:207 (1998).
16. J. L. Souquet, M. Duclot, and M. Levy, *Solid State Ionics* **105**:237 (1998).
17. E. Caillot, M. J. Duclot, J. L. Souquet, and M. Levy, *Phys. Chem. Glasses* **35**:22 (1994).